Naunyn-Schmiedeberg's Archives of Pharmacology (2021) 394:261–277
https://doi.org/10.1007/s00210-020-01972-5

ORIGINAL ARTICLE

Melatonin alleviates sepsis-induced heart injury through activating the Nrf2 pathway and inhibiting the NLRP3 inflammasome

Ibtissem Rahim[1,2,3] · Ramy K. Sayed[1,4] · Marisol Fernández-Ortiz[1] · Paula Aranda-Martínez[1] · Ana Guerra-Librero[1] · José Fernández-Martínez[1] · Iryna Rusanova[1] · Germaine Escames[1,5] · Bahia Djerdjouri[3] · Darío Acuña-Castroviejo[1,5]

Received: 23 April 2020 / Accepted: 31 August 2020 / Published online: 16 September 2020

Abstract

Melatonin improved the outcome of septic cardiomyopathy by inhibiting NLRP3 priming induced by reactive oxygen species. To get insights into these events, we studied the melatonin/Nrf2 antioxidant pathways during sepsis in the heart of NLRP3-deficient mice. Sepsis was induced by cecal ligation and puncture and melatonin was given at a dose of 30 mg/kg. Nuclear turnover of Nrf2 and p-Ser40 Nrf2 and expression of *ho-1* were enhanced in $nlrp3^{+/+}$ and $nlrp3^{-/-}$ mice during sepsis. Sepsis caused higher mitochondria impairment, apoptotic and autophagic events in $nlrp3^{+/+}$ mice than in $nlrp3^{-/-}$ animals. These findings were accompanied by greater levels of Parkin and PINK-1, and lower Mfn2/Drp-1 ratio in $nlrp3^{+/+}$ than in $nlrp3^{-/-}$ mice during sepsis, supporting less mitophagy in the latter. Ultrastructural analysis of myocardial tissue further confirmed these observations. The activation of NLRP3 inflammasome accounted for most of the deleterious effects of sepsis, whereas the Nrf2-dependent antioxidative response activation in response to sepsis was unable to neutralize these events. In turn, melatonin further enhanced the Nrf2 response in both mice strains and reduced the NLRP3 inflammasome activation in $nlrp3^{+/+}$ mice, restoring myocardial homeostasis. The data support that the anti-inflammatory efficacy of melatonin against sepsis depends, at least in part, on Nrf2 activation.

Keywords NLRP3 deficiency · Nrf2 · Sepsis · Melatonin · Apoptosis · Mitochondria

Introduction

Septic cardiomyopathy is a common cause of death in intensive care units (Hunter and Doddi 2010; Zador et al. 2019). Defined as an exaggerated systemic inflammatory response to infection, sepsis remains a prevalent clinical challenge with poorly understood pathophysiology. A substantial body of evidence supports various factors in the development of cardiac dysfunction during sepsis. Among them, reactive oxygen (ROS) and nitrogen (RNS) species, mitochondrial dysfunction, inflammatory signaling, and cell death are activated during sepsis (Ortiz et al. 2014; Alvarez et al. 2016; Neri et al. 2016).

NF-κB activation and subsequent oxidative stress caused by excessive ROS/RNS are the initiating pathophysiological steps of sepsis (Wheeler 2011). The uncontrolled ROS generation impairs mitochondrial structure and biogenesis via oxidative modifications on macromolecules, such as mitochondrial DNA (mtDNA) and directly inhibits oxidative phosphorylation (Singer 2014). Impaired mitochondria release various danger signals including ROS and mtDNA sensed by NLRP3

Electronic supplementary material The online version of this article (https://doi.org/10.1007/s00210-020-01972-5) contains supplementary material, which is available to authorized users.

✉ Darío Acuña-Castroviejo
dacuna@ugr.es

[1] Departamento de Fisiología, Facultad de Medicina, Instituto de Biotecnología, Centro de Investigación Biomédica, Parque Tecnológico de Ciencias de la Salud, Universidad de Granada, 18016 Granada, Spain

[2] Département de Biologie et Physiologie Cellulaire, Faculté des Sciences de la Nature et de la Vie, Université Blida 1, 09000 Blida, Algeria

[3] Faculté des Sciences Biologiques, Laboratoire de Biologie Cellulaire et Moléculaire, Université des Sciences et de la Technologie Houari Boumediene, Bab-Ezzouar, 16111 Algiers, Algeria

[4] Department of Anatomy and Embryology, Faculty of Veterinary Medicine, Sohag University, Sohag 82524, Egypt

[5] CIBERfes, Ibs.Granada, and UGC de Laboratorios Clínicos, Complejo Hospitalario de Granada, 18016 Granada, Spain

inflammasome (Zhou et al. 2011; Ortiz et al. 2014). Recent studies suggested the critical role of NLRP3 inflammasome in the initiation and the exacerbation of the inflammatory response during sepsis in the mouse heart (Garcia et al. 2015; Volt et al. 2016). Upon activation, NLRP3 forms a multiprotein complex activating a caspase-1 that maturates pro-cytokines including pro-IL-1β to their mature forms, boosting inflammation (Latz et al. 2013). Enhanced ROS and mitochondrial damage triggers apoptotic and/or autophagy/mitophagy events to remove dysfunctional mitochondria (Li et al. 2015, 2019a).

The resolution of mitochondrial oxidative stress and the inflammatory response requires a key transcription factor, Nrf2 (nuclear factor E2-related factor 2) that plays an essential role in the regulation of redox homeostasis, cytoprotective defense, and inflammatory responses (Kensler et al. 2007; Lu et al. 2016; Ahmed et al. 2017). Nrf2 forms an inactive complex with its cytosolic repressor Kelch-like ECH associated protein 1 (Keap1), which in turn mediates proteasomal degradation of Nrf2 (Tong et al. 2006). In response to inflammation or oxidative stress, Keap1 dissociates from Nrf2 that translocases into the nucleus and binds to an antioxidant response element (ARE), transcribing its target genes involved in protection against xenobiotics and oxidative stress; these include many antioxidant and phase II detoxifying genes, including γ-glutamyl cysteine synthase, glutathione peroxidase (GPx), glutathione reductase (GRd), and superoxide dismutase (SOD) and heme oxygenase 1 (Kensler et al. 2007; Magesh et al. 2012; Tu et al. 2019), which exert significant antioxidant, anti-inflammatory, and anti-apoptotic effects, protecting the heart from pathological conditions (Yeh et al. 2016). Nrf2 and NLRP3 inflammasome have a complex relationship; whereas the Nrf2 pathway could inhibit NLRP3 inflammasome activation in sepsis (Loboda et al. 2016), other authors reported that Nrf2 is a positive regulator of NLRP3, although Nrf2 activation can inhibit the inflammasome activation. In turn, NLRP3 may inhibit Nrf2 via Keap1-dependent degradation (Garstkiewicz et al. 2017). Thus, although Nrf2 activation can improve survival during experimental sepsis (Kong et al. 2011; Lambertucci et al. 2017), the Nrf2/NLRP3 inflammasome connection remains unclear.

Melatonin (N-acetyl-5-methoxytryptamine, aMT) is an outstanding endogenous antioxidant and anti-inflammatory molecule that protects mitochondria from oxidative damage (Crespo et al. 1999; Martin et al. 2000; Escames et al. 2003; Ortiz et al. 2014). The downregulation of the NF-κB/NLRP3 inflammasome connection by melatonin during sepsis in mouse cardiomyocytes has been recently reported (Garcia et al. 2015; Volt et al. 2016), suggesting that the NLRP3 inflammasome could be a specific target of melatonin (Rahim et al. 2017). In addition, melatonin possesses anti-apoptotic properties which are related to mitochondrial protection (Zhao et al. 2015). These effects link melatonin's actions with the Nrf2 pathway, a connection recently supported by the upregulation of Nrf2 expression and activation of its antioxidant-related products by melatonin (Santofimia-Castano et al. 2015; Vriend and Reiter 2015).

Together, these data suggest a connection between melatonin, Nrf2, and NLRP3 inflammasome, orchestrating mitochondrial homeostasis during sepsis. This study therefore aimed to evaluate whether the protective effect of melatonin by inhibiting NLRP3 inflammasome requires Nrf2 activation. Thus, we considered it worthwhile to analyze the melatonin/Nrf2/NLRP3 connection in wild-type and NLRP3-deficient mice during sepsis in mouse cardiomyocytes.

Materials and methods

Chemicals

Melatonin (N-acetyl-5-methoxytryptamine, aMT) was purchased from FAGRON (Venecoweg, Nazareth, Belgium), PEG was purchased from VWR (Radnor, PA, USA), and Bradford was purchased from Bio-Rad (Hercules, CA, USA). All other chemicals, of the purest available grade, were obtained from Sigma-Aldrich (St. Louis, MO, USA) unless otherwise specified.

Animals

All experiments were performed on healthy adult 3-month-old female wild-type C57BL/6J and *nlrp3*$^{-/-}$ (B6.129S6-Nlrp3^{tm1Bhk}/J) mice weighing between 22 and 25 g. Female wild-type (*nlrp3*$^{+/+}$) C57BL/6 and *nlrp3*$^{-/-}$ mice on the C57BL/6J background (> 10 backcrosses) were purchased from Harlan Laboratories (Barcelona, Spain) and The Jackson Laboratory (Bar Harbor, ME, USA), respectively. No differences between female and male mice were detected in previous experiments; moreover, previous experiments with the same experimental paradigm were also performed in females (Rahim et al. 2017). Mice were housed in the animal facility of the University of Granada under a specific pathogen-free barrier facility, with a controlled 12-h light/dark cycle (lights on at 08:00 h) at 22 °C ± 1 °C, and free access to tap water and rodent chow. This study was performed according to the National Institutes of Health Guide for the Care and Use of Laboratory Animals (National Research Council, National Academy of Sciences, Bethesda, MD, USA), the European Convention for the Protection of Vertebrate Animals used for Experimental and Other Scientific Purposes (CETS # 123), and the Spanish law for animal experimentation (R.D. 53/2013). The final study was approved by the Andalusian's Ethical Committee (protocol number: 462-CEEA-2013) (Spain). ARRIVE guidelines were consulted for the study.

Surgical procedures and melatonin treatment

Sepsis was induced by cecal ligation and puncture (CLP) (Rittirsch et al. 2009). Briefly, after being anesthetized with Equithesin (1 mL/kg, intraperitoneal), mice were put on an aseptic operating table. In a sterile operation environment, a 1-cm midline incision was made to expose the cecum. Next, to obtain the same septic severity, the cecum was tightly ligated below the ileocecal valve with 4-0 silk suture, and then punctured three times with a 22-gauge needle. A small amount of stool was gently squeezed through the puncture site. The cecum was replaced into the peritoneal cavity, and the abdominal incision was then stitched in two layers. All mice underwent surgery at the same time of the day, i.e., 08:00–10:00 a.m. to avoid diurnal variations on the immune response, and they were sacrificed 8 h after CLP. Both *nlrp3*$^{+/+}$ and *nlrp3*$^{-/-}$ animals were grouped ($n = 6$ animals/group) as follows: C, control group; S, septic group, and S+aMT (S+Melatonin), septic group treated with melatonin. The S+aMT group received 3 doses of 30 mg/kg melatonin each dissolved in 30% PEG (Ortiz et al. 2014) with the following schedule: one intraperitoneal injection 30 min before surgery, a second subcutaneous injection just after surgery, and the third subcutaneous injection was done 4 h after surgery. Animals were euthanized 8 h after CLP and the hearts were rapidly removed, washed in cold saline, and processed for fraction extraction (cytosol and nucleus), mitochondrial isolation or freshly fixed for ultrastructure and fluorescence, or stored at − 80 °C for further analysis.

Isolation of cytosol, nuclear, and mitochondrial fractions for western blot analysis

Pure cytosol, nuclear, and mitochondrial fractions were prepared from fresh tissue with some modifications (Dimauro et al. 2012). Briefly, heart tissue was homogenized on ice at 800 rpm in 500 μL of STM buffer containing 250 mM sucrose, 50 mM Tris–HCl pH 7.4, 5 mM $MgCl_2$, 0.5 mM DTT, 5% phosphatase inhibitor buffer (125 mM NaF, 250 mM β-glycerophosphate, 250 mM *p*-nitrophenyl phosphate, and 25 mM $NaVO_3$), and a protease inhibitor cocktail using an SS2 stirrer with a Teflon pestle (Stuart Scientific Co. Ltd., Cambridge, UK). The homogenate was decanted into a centrifuge tube and maintained on ice for 30 min, vortexed at maximum speed for 15 s and then subjected to serial centrifugations. First, the homogenate was centrifuged at 800*g* for 15 min; the resulting supernatant was centrifuged again at 800*g* for 10 min; the resulting pellet was combined with the first pellet for isolation of nuclear fractions. The cytosolic fraction was obtained from the supernatant centrifugation at 11,000*g* for 10 min which thereafter precipitated in 100% acetone at − 20 °C for at least 1 h followed by centrifugation at 12,000*g* for 5 min and the resulting pellet was then resuspended in 300 μL STM buffer. For nuclear extraction, the pellet was gently resuspended in 500 μL STM buffer, vortexed at maximum speed for 15 s, and washed twice at 500*g* for 15 min and at 1000*g* for 15 min. After centrifugation, the pellet was resuspended by gentle pipetting in 500 μL NET buffer (comprising 20 mM HEPES pH 7.9, 1.5 mM $MgCl_2$, 0.5 M NaCl, 0.2 mM EDTA, 20% glycerol, 1% Triton-X-100, 0.5 mM DTT, protease and phosphatase inhibitors) and then vortex and incubated on ice for 30 min. After incubation, the mixture containing the nuclei was sonicated on ice for 3 × 10 s and the lysate was then centrifuged at 9000*g* for 30 min. The resulting supernatant was the final nuclear fraction. All procedures were carried out at 4 °C. The cytosolic and nuclear fractions were aliquoted and frozen at − 80 °C until analyzed (Dimauro et al. 2012). The pure mitochondrial fraction was obtained from the supernatant of cytosolic fraction, by differential centrifugation and Percoll density gradient (Escames et al. 2003). The mitochondrial pellets obtained from the centrifugation at 11,000*g* for 10 min was resuspended at 4 °C in Buffer A (5 mM HEPES, 250 mM mannitol, 0.5 mM EGTA, 0.1% free fatty acids albumin, BSA, pH 7.4), and poured in ultracentrifuge tubes containing buffer B (25 mM HEPES, 225 mM mannitol, 1 mM EGTA, 0.1% BSA, pH 7.4, at 4 °C) and Percoll. The mixture was centrifuged at 95,000*g* for 30 min at 4 °C. The fraction with a density of 1.052–1.075 g/mL, corresponding to a pure mitochondrial fraction, was collected, washed twice with buffer A at 10,300*g* for 10 min at 4 °C to remove the Percoll, resuspended and sonicated (3 × 10 s with 30-s pauses 3 × 10 s with 30-s pauses) on ice in SOL buffer (50 mM Tris–HCl pH 6.8, 1 mM EDTA, 0.5% Triton-X-100, 0.5 mM DTT5% phosphatase inhibitor buffer a protease inhibitor cocktail), and stored at − 80 °C until western blot analysis was performed. The purity of the mitochondrial fraction obtained with this experimental procedure has been previously validated (López et al. 2006). The protein content of each compartment was quantified using the Bradford protein assay (Bradford 1976).

Western blot analysis

Nuclear, cytosol, or mitochondrial proteins (20–40 μg) were separated by SDS-PAGE on 12 or 15% acrylamide gels under denaturing conditions and then transferred onto polyvinylidene difluoride (PVDF, Millipore, Seville, Spain) membranes. The membranes were blocked with 5% nonfat milk or 5% BSA in PBST and then incubated overnight at 4 °C with primary antibodies. Then, membranes were washed with PBST, incubated with the appropriate secondary antibodies for 1 h at room temperature, and washed again with PBST. The protein bands were detected with the Western Lightning Plus-ECL system (Perkin Elmer, S.L., Madrid, Spain). Plots were digitized on a Kodak Image Station 2000R and quantified with 1D Image Analysis software 3.6 (Eastman Kodak Co., Rochester, NY, USA). Protein band intensity was normalized to GAPDH, histone 3,

and VDAC for cytosol, nucleus, and mitochondria, respectively, and the data expressed in terms of percent relative to control. The following primary antibodies were used: Nrf2, sc-722; Bcl-2, sc-492; Bax, sc-526; p53, sc-6243; caspase 3, sc-7148; Mfn-2, sc-50331; Drp-1,sc-32898; GAPDH, sc-25778; histone3, sc-8654, from Santa Cruz Biotechnology (Quimigen, Madrid, Spain); phosphor Ser-40 Nrf2, bs-2013R from Bioss (Atlanta, GA, USA), Keap1, 10503-2-AP and p62/SQSTM1, 18420-1-AP from Proteintech (Manchester, UK); Parkin, ab15954 and VDAC1, ab14734 from Abcam (Cambridge, USA); PINK1, 10006283 from Cayman Chemical (Ann Arbor, MI, USA) and LC3I/II, NB100-2220 from Novus biological (Novusbio, Centennial, CO, USA). Anti-rabbit (dilution 1:5000; Thermo Fisher Scientific, Madrid, Spain), anti-mouse (dilution 1:1000; Becton Dickinson S.A., Madrid, Spain), and anti-goat (dilution 1:1000; Santa Cruz Biotechnology) horseradish peroxidase-conjugated secondary antibodies were used according to the manufacturer's instructions.

Real-time quantitative PCR

Total RNA was isolated with the NZY Total RNA Isolation kit (Nzytech Gene & Enzymes, Lisbon, Portugal), and reverse transcription was performed with the qScriptTM cDNA SuperMix kit (Quanta Biosciences, VWR International Eurolab S.L., Madrid, Spain). The quantity and quality of RNA were determined in a NanoDrop by 260:280-nm ratio absorbance and gel electrophoresis, respectively. Quantitative reverse transcription polymerase chain reaction (qRT-PCR) was performed in a Stratagene Mx3005P QPCR System (Agilent Technologies, Barcelona, Spain) with the iTaq SYBR Green Supermix (Bio-Rad Life Sciences, Madrid, Spain). Primer sequences of targeted genes were designed using the Beacon Designer software (Premier Biosoft Inc., Palo Alto, CA, USA), (Supplementary Table 1), and output data were analyzed with the MxPro QPCR software (v 4.0) (Agilent Technologies) according to the standard curves generated from increasing amounts of cDNA (0.05, 0.5, 5, 50, and 500 ng). The PCR program was initiated with 10 min at 95 °C before 40 thermal cycles, each consisting of 15 s at 95 °C and 1 min at 55 °C. *Beta-actin* housekeeping was used as an endogenous reference gene; a no template-free (water) reaction was used as negative control to determine any contamination, and untreated *nlrp3*$^{+/+}$ was used as a calibrator sample. Supplementary Table 1 shows the sequences of gene-specific primers used in this study.

Measurement of antioxidant enzyme activity

All enzyme activities were assessed in cytosolic fractions. Catalase activity (U/mg prot) was measured following the decomposition of H_2O_2 at 240 nm according to Aebi's method (Aebi 1984). Cu/Zn superoxide dismutase (SOD-1) activity (U/mg prot) was assayed in terms of its ability to inhibit the auto-oxidation of adrenalin to adrenochrome at pH 10.2 (Misra and Fridovich 1972). Glutathione reductase (GRd) and glutathione peroxidase (GPx) activities (nmoL/min mg prot) were measured by determining spectrophotometrically the NADPH oxidation for 3 min at 340 nm (Jaskot et al. 1983), using a UV spectrophotometer (Shimadzu Deutschland, GmbH, Duisburg, Germany). In both cases, non-enzymatic NADPH oxidation was subtracted from the overall rates. Protein concentration in the samples was determined spectrophotometrically with the Bradford reagent (Bradford 1976).

Mitochondrial respiration assessment

Heart mitochondria were freshly prepared as described (Rogers et al. 2011), with slight modifications. Briefly, hearts were washed and submerged in 1 mg/mL of proteinase K solution for 30 s. Then, the heart was minced and homogenized on ice at 800 rpm in (1:10, w/v) isolation buffer (250 mM sucrose, 2 mM EDTA, 10 mM Tris, 0.5% free fatty acid albumin (BSA), pH 7.4) at 4 °C using an SS2 homogenizer with a Teflon pestle (Stuart Scientific Co. Ltd., Cambridge, UK). The homogenate was centrifuged twice at 1000*g* for 5 min at 4 °C, and the resulting supernatant was centrifuged at 23,000*g* for 10 min at 4 °C. The mitochondrial pellet was then resuspended in 100 μL of isolation buffer without BSA, and a 10-μL aliquot was used for Bradford protein quantitation. The remaining sample was washed with 900 μL of isolation buffer without BSA and centrifuged at 13,000*g* for 3 min at 4 °C. The final crude mitochondrial pellet was resuspended in 90 μL MAS 1× medium containing 70 mM sucrose, 220 mM mannitol, 10 mM KH2PO4, 5 mM MgCl2, 2 mM HEPES, 1 mM EGTA, and 0.2% (w/v) fatty acid-free BSA, pH 7.2.

Mitochondrial respiration was measured by using an XFe24 Extracellular Flux Analyzer (Seahorse Bioscience) (Rogers et al. 2011). Mitochondria were first diluted to the needed concentration required for plating in cold 1× MAS (2 μg/well). Next, 50 μL of the diluted mitochondria (2 μg/well in ice 1× MAS) was filed in XF plate (except for background correction wells) and centrifuged at 2000*g* for 10 min at 4 °C. After centrifugation, 450 μL of the substrate containing 1× MAS + substrate (10 mM succinate, 2 mM malate, 2 mM glutamate, and 10 mM pyruvate) was added to each well and 500 μL in the background correction wells. Respiration by the mitochondria was sequentially measured in a coupled state with substrate present State 2 (basal respiration), followed by State 3 (phosphorylating respiration, in the presence of ADP and substrate), State 4o (non-phosphorylating or resting respiration induced with the addition of oligomycin when all ADP was consumed), and then State 3μ (maximal uncoupler-stimulated respiration). This allows respiratory control ratios (RCR; State 3/State 4o, or State

3μ/State 4o) to be assessed. Injections were as follows: port A, 50 μL of 40 mM ADP (4 mM final), 55 μL of 30 μg/mL oligomycin (3 μg/mL final), 60 μL of 40 μM FCCP (5 μM final), and 65 μL of 40 μM antimycin A (4 μM final). All data were expressed in pmol/min/μg protein.

Transmission electron microscopy

Small specimens of cardiac muscle fibers of both *nlrp3*$^{+/+}$ and *nlrp3*$^{-/-}$ mice were dissected from left ventricles of experimental groups ($n = 3$ animals/group) and were fixed freshly in a 2.5% glutaraldehyde in 0.1 M cacodylate buffer (pH 7.4). The samples were postfixed in 0.1 M cacodylate buffer with 1% osmium tetroxide and 1% potassium ferrocyanide for 1 h., immersed on 0.15% tannic acid for 50 s, incubated in 1% uranyl acetate for 1.5 h. and dehydrated in ethanol. Specimens were then embedded in resin and ultrathin sections were cut by a Reichert-Jung Ultracut E ultra-microtome, stained with uranyl acetate and lead citrate (Reynolds 1963), and examined on a Carl Zeiss Leo 906E electron microscope. Morphometrical analyses of left ventricle ultrastructure including number and cross-section area (CSA) of intermyofibrillar mitochondria (IFM) were performed on the transmission electron microscopy (TEM) images (area measured 7.79-μm width and 5.93-μm height) of the experimental animal groups using ImageJ processing software. These morphometrical studies were conducted by two double-blinded operators, comparing data obtained subsequently. The measurements were carried out on 5 randomly selected sections per animal, with 5 different areas were measured from each section.

Hoechst 33258 nuclear staining for the detection of apoptosis

Hoechst 33258 fluorescent dye was used for the detection of cardiac apoptosis through staining the nuclei and determining those with chromatin condensation and nuclear fragmentation (Latt et al. 1975). Cardiac sections were dissected from left ventricles of the experimental group ($n = 3$ animals/group). The sections were formalin-fixed and paraffin-embedded. Multiple sections (4 μm) were deparaffinized with xylene, stained with 1 g/mL Hoechst 33258 for 30 min at room temperature in darkness, and rinsed with PBS thrice, 5 min each. The sections were air-dried, mounded, and observed under fluorescence microscopy (excitation/emission wavelength 350/460 nm) for apoptotic fragmented nuclei. Detection of apoptotic nuclei ratio was performed on digitally acquired images by two double-blinded operators. Analysis of the apoptotic nuclei ratio was conducted on 15 randomly selected sections per animal, with 5 different areas were measured from each section.

Statistics

Data are expressed as mean ± SEM. GraphPad Prism v. 6.0 (GraphPad Software, Inc., La Jolla, CA, USA) was used to analyze data. Normal distribution of the data was assessed by the D'Agostino-Pearson normality test before to apply one-way ANOVA with a Tukey's post hoc test were used to compare the differences between experimental groups. $P < 0.05$ was considered to be statistically significant.

Results

The absence of NLRP3 does not affect the turnover of Nrf2 in the heart of mice, which is further enhanced by melatonin

Previous studies suggested an inhibitory effect of Nrf2 on NF-κB-dependent gene expression in sepsis (Kong et al. 2011). Our data demonstrated the effects of sepsis in the NF-κB activation, in terms of *tnf-α*, *pro-il-1β*, and *nlrp3* expression, which were more significantly induced in *nlrp3*$^{+/+}$ than in *nlrp3*$^{-/-}$ mice and blunted by melatonin, which also blocks the *nlrp3* expression in wild-type mice (Suppl. Fig. 1A). We also reported an increase of *nampt* and *sirt-1* gene expression in *nlrp3*$^{+/+}$ but not in *nlrp3*$^{-/-}$ mice during sepsis, which was further enhanced by melatonin (Suppl. Fig. 1B).

The significance of Nrf2 in NLRP3 inflammasome activation, however, has not been fully characterized. Our results show that sepsis increased Nrf2 signaling through the induction of Nrf2 mRNA and protein production, and the phosphorylation of the latter to pSer40-Nrf2, facilitating its nuclear translocation. Both, Nrf2 and pSer40-Nrf2, enter in the nucleus and reduced their cytosolic levels to the same extent in *nlrp3*$^{+/+}$ and *nlrp3*$^{-/-}$ mice (Fig. 1a–c and e) (Gallego-Selels et al. 2020). Melatonin treatment further increased *nrf2* expression and nuclear protein content of Nrf2 and pSer40-Nrf2 in wild-type and mutant mice (Fig. 1a–c and e), suggesting that it may mediate its antioxidant activity in part through the modulation of the Nrf2/ARE signaling pathway. Keap1 protein content in the cytosol was significantly reduced during sepsis in *nlrp3*$^{+/+}$ and *nlrp3*$^{-/-}$ mice, and it was not modified by melatonin, whereas *keap1* mRNA remained unchanged (Fig. 1d and f).

The absence of NLRP3 reduces the antioxidant response to sepsis in the heart of mice, which is upregulated by melatonin

We next asked whether the antioxidant response during sepsis could be affected by NLRP3 inflammasome deficiency, analyzing the expression and activity of the main antioxidant

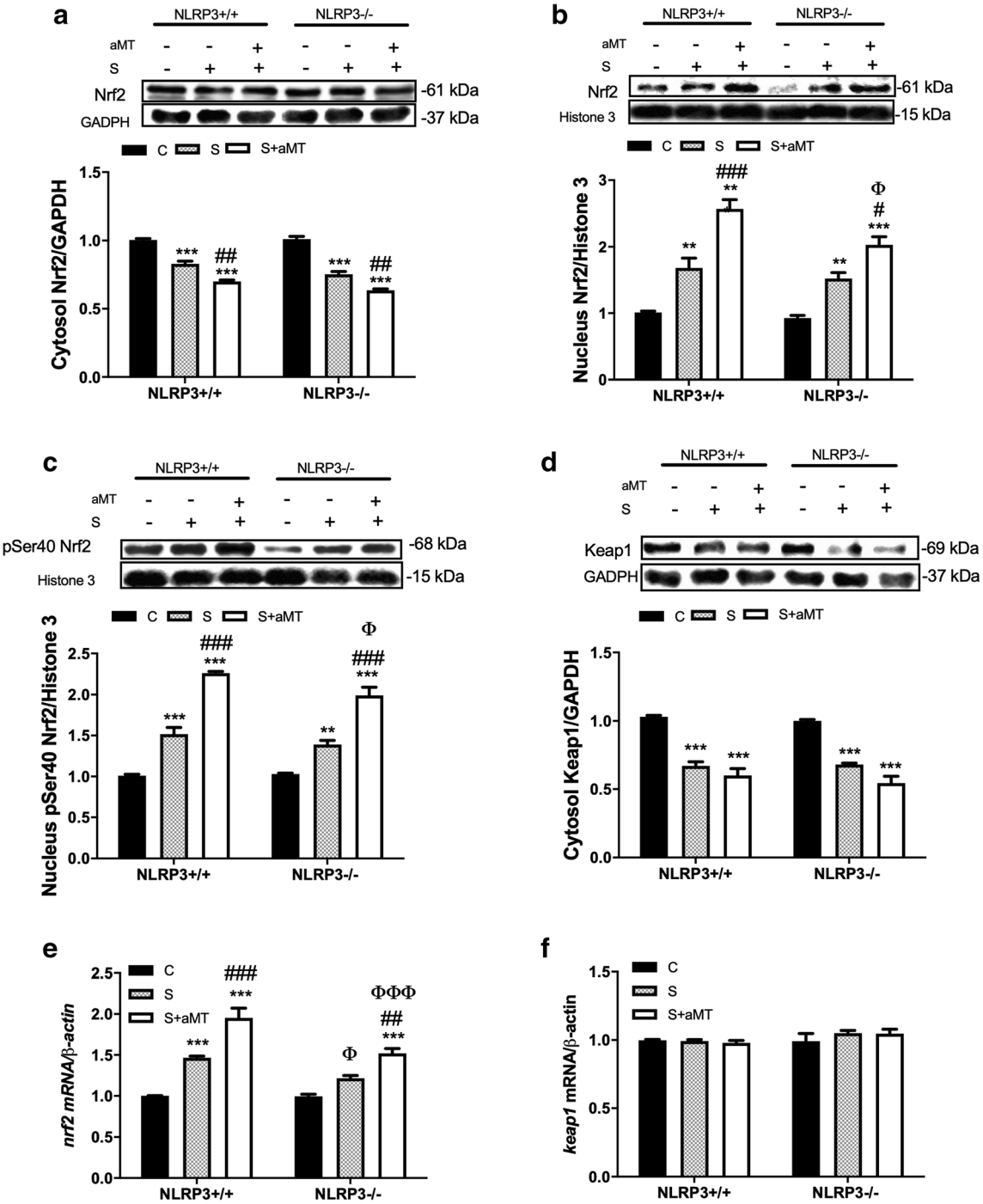

Fig. 1 Changes in Nrf2 turnover in mice. Experiments were performed in hearts of control and septic *nlrp3*$^{+/+}$ and *nlrp3*$^{-/-}$ mice, with or without melatonin treatment. mRNA expression (qRT-PCR), and cytosolic and nuclear protein content (western blot) for *nlrp3*$^{+/+}$ and *nlrp3*$^{-/-}$ mice are shown. **a** Changes in cytosolic Nrf2 protein content. **b** Nuclear Nrf2 protein content. **c** Nuclear protein content of pSer40 Nrf2. **d** Cytosolic levels of Keap1 protein. **e** mRNA levels of *nrf2*. **f** mRNA levels of *keap1*. Data are expressed as mean ± SEM of $n = 6$ animals/group. C, control; S, sepsis; and S+aMT, septic animals treated with 3 × 30 mg//kg melatonin. $^{**}p < 0.01$ and $^{***}p < 0.001$ *v.* C; $^{\#}p < 0.05$, $^{\#\#}p < 0.01$, and $^{\#\#\#}p < 0.001$ *v.* S; $^{\Phi}p < 0.05$, and $^{\Phi\Phi\Phi}p < 0.001$ *v. nlrp3*$^{+/+}$

enzymes which are also members of the Nrf2-downstream target genes. Although we observed a significant increase in the first (SOD) and second (GPx) lines of the antioxidative defense (Fig. 2a), the decline in GRd activity and the absence of catalase changes, revealed a reduced antioxidant capacity during sepsis in *nlrp3*$^{+/+}$ mice (Fig. 2a). This response may explain, at least in part, the uncontrolled oxidative stress taking place during sepsis. Mice lacking NLPR3 showed a reduction in basal SOD, GPx, and GRd activities, and an elevation in catalase activity (Fig. 2a). Unlike *nlrp3*$^{+/+}$, *nlpr3*$^{-/-}$

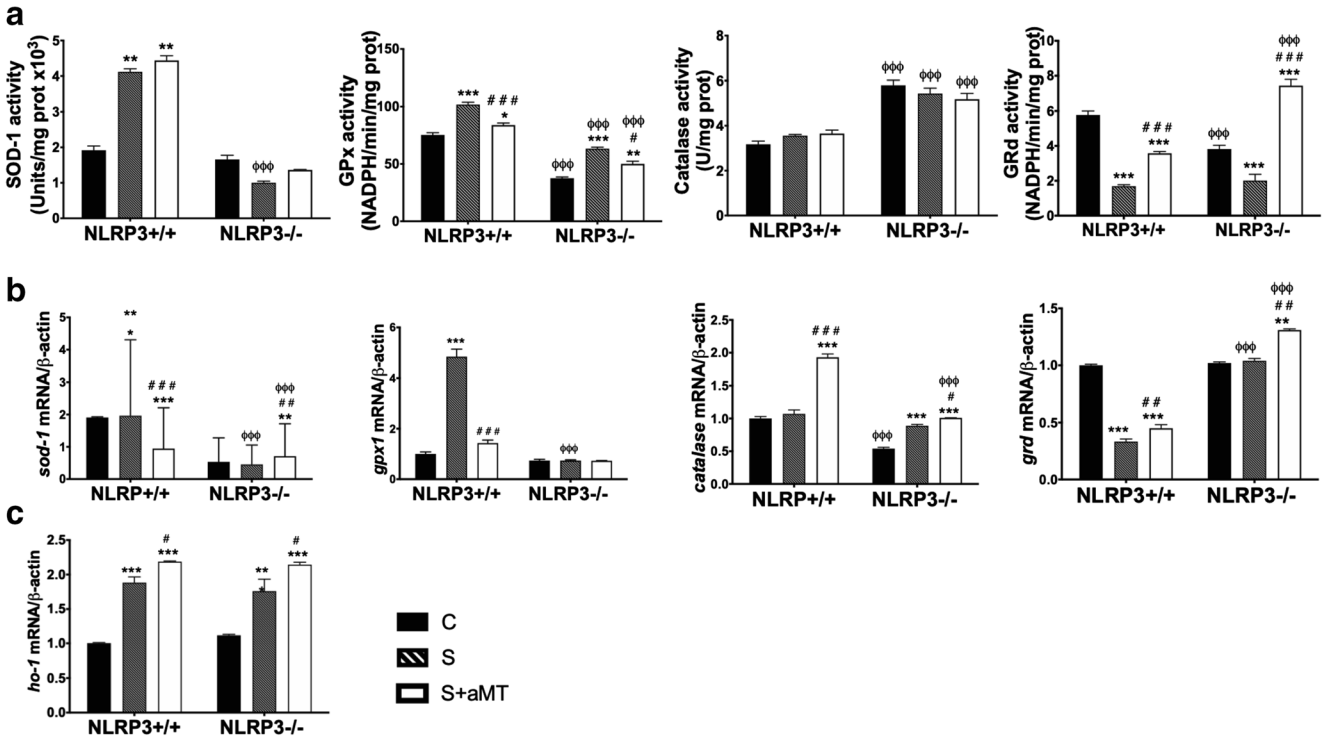

Fig. 2 Changes in the antioxidant response against sepsis in mice. Experiments were performed in heart of control and septic *nlrp3*$^{+/+}$ and *nlrp3*$^{-/-}$ mice, with or without melatonin treatment. **a** Activities of SOD-1, GPx, catalase, and GRd. **b** mRNA expression of *sod-1*, *gpx*, *catalase*, and *grd*. **c** mRNA expression of *ho-1*. Data are expressed as mean ± SEM of $n = 6$ animals/group. C, control, S; sepsis; S+aMT, septic animals treated with 3 × 30 mg/kg melatonin. $^{*}p < 0.05$ and $^{***}p < 0.001$ *v.* C; $^{\#}p < 0.05$ and $^{\#\#\#}p < 0.001$ *v.* S; $^{\Phi}p < 0.05$, $^{\Phi\Phi}p < 0.01$, and $^{\Phi\Phi\Phi}p < 0.001$ *v. nlrp3*$^{+/+}$

septic mice exhibited a reduction in SOD and GRd activities, whereas GPx activity increased and catalase did not change (Fig. 2a). The mRNA expression of these antioxidant enzymes generally paralleled their activity changes except for catalase and, especially, GRd (Fig. 2b). Besides the expression of *grd* in *nlpr3*$^{-/-}$ mice under sepsis, the enzyme activity declined significantly, a finding related to the oxidative damage of this enzyme (Huang and Philbert 1996). The data suggest that *nlpr3*$^{-/-}$ mice trigger a lower antioxidative defense than *nlrp3*$^{+/+}$ mice, which is in line with a reduced inflammatory response in these mice elsewhere reported (Rahim et al. 2017).

Melatonin treatment generally did not modify the effects of sepsis on the activity of the antioxidant enzymes except for the increase in GRd and a reduction in GPx in mutant mice (Fig. 2a). Furthermore, melatonin reduced the expression of *sod-1* and *gpx*, and increased that of *cat* and *grd* in *nlrp3*$^{+/+}$ mice, whereas it stimulated the expression of all of them except for *gpx* in *nlpr3*$^{-/-}$ mice (Fig. 2b). Thus, melatonin modulates the antioxidant response as a function of the environmental oxidative stress and maintains the GSH pool in the cell through the activation of GRd (Escames et al. 2007).

In response to enhanced Nrf2, septic mice exhibited an increased expression of the inducible phase II detoxifying enzyme *ho-1* in both mouse strains; this effect was further enhanced by melatonin (Fig. 2c). Thus, the modulation of Nrf2/HO-1 response seems to be one of the targets of melatonin during sepsis, and it is independent of the NLRP3 inflammasome activation.

The absence of NLRP3 reduces the mitochondrial respiration impairment to sepsis in the heart of mice, which is counteracted by melatonin

Mitochondrial impairment and bioenergetic failure have been related to the pathogenesis of myocardial injury during sepsis (Escames et al. 2007; Doerrier et al. 2016). We investigated here whether NLRP3 inflammasome deficiency affects the mitochondrial bioenergetic failure in sepsis. Our results show that sepsis induced a more significant decrease in the phosphorylating respiration (State 3) in *nlrp3*$^{+/+}$ mice than in *nlrp3*$^{-/-}$ mice (Fig. 3b). Basal respiration (State 2) was also reduced in *nlrp3*$^{+/+}$ but not in *nlrp3*$^{-/-}$ mice (Fig. 3a), whereas State 4o was not modified (Fig. 3c). Maximal uncoupler-stimulated respiration (State 3μ), respiratory control ratio (RCR; State 3/State 4o), and ATP production decrease in *nlrp3*$^{+/+}$ mice but not in mutant mice during sepsis (Fig. 3d, e, and g). Proton leak increased in *nlrp3*$^{+/+}$ mice but not in mutant mice during sepsis (Fig. 3f). Melatonin administration counteracted these negative

effects of sepsis, restoring the control values of the mitochondrial respiratory states, RCR, and the ability of mitochondria to produce ATP in *nlrp3*$^{+/+}$ mice (Fig. 3).

Ultrastructural changes of cardiomyocytes during sepsis and the prophylactic effect of melatonin administration in the heart of mice

Transmission electron microscopy of the cardiac muscle fibers of *nlrp3*$^{+/+}$ mice revealed the normal cardiomyocyte ultrastructure, which is composed of centrally located nucleus (N), well-organized longitudinally arranged myofibrils (Mf) giving the longitudinal striations of cardiac muscle, and each one constitutes of thread-like actin and myosin myofilaments. The sarcomeres (S) are well-alignment between each two successive Z-lines. The intermyofibrillar spaces present mitochondria and sarcoplasmic reticulum (SR), the former with compacted cristae and gathered in clusters in-between cardiac myofibrils as intermyofibrillar mitochondria (M) (Suppl. Fig. 2A). *nlrp3*$^{-/-}$ mice showed the normal architecture of the cardiomyocytes with more abundant and large-sized intermyofibrillar mitochondria than *nlrp3*$^{+/+}$ mice. These mitochondria were gathered in different orientations and clusters among the myofibrils, and were compacted with well-arranged cristae (Suppl. Fig. 2D). Morphometrical analysis revealed that the number of intermyofibrillar mitochondria (IFM) of cardiomyocytes in *nlrp3*$^{+/+}$ mice was 22.4 ± 1.3, while that of *nlrp3*$^{-/-}$ mice was 30.8 ± 2.4 (Suppl. Fig. 2G). The cross-section area (CSA) of IFM of *nlrp3*$^{+/+}$ and *nlrp3*$^{-/-}$ mice were 0.69 ± 0.06 μm2 and 0.84 ± 0.09 μm2 respectively (Suppl. Fig. 2H).

During sepsis, the cardiomyocytes of *nlrp3*$^{+/+}$ mice demonstrated signs of degeneration, where the actin and myosin myofilaments of myofibrils were ill distinct (black asterisk). Misalignments of adjacent sarcomeres were detected with reduction of mitochondrial number (19.4 ± 1.6) and size (0.45 ± 0.04 μm^2). The presence of numerous mitochondria vacuolated with disorganized cristae (white arrow) and accumulations of glycogen droplets (G) were also demonstrated (Suppl. Fig. 2B and G). However, *nlrp3*$^{-/-}$ mice showed less degree of damage during sepsis than *nlrp3*$^{+/+}$ mice. The myofibrils were normally organized and the myofilaments were well-aligned. Most of the intermyofibrillar mitochondria were compacted and the cristae were organized, although, individual mitochondria revealed destructed cristae and small vacuoles. Similar to *nlrp3*$^{+/+}$ mice, excessive glycogen droplets were illustrated peripherally beneath the sarcolemma (black arrow) (Suppl. Fig. 2E). The number of IFM in the septic *nlrp3*$^{-/-}$ mice was 28.2 ± 1.5, and the CSA was 0.39 ± 0.03 μm^2 (Suppl. Fig. 2G and H).

Melatonin administration to *nlrp3*$^{+/+}$ and *nlrp3*$^{-/-}$ mice preserved the normal structure of the cardiac fibers and alignment of the myofilaments, and maintained the integrity of the intermyofibrillar mitochondria number (29.4 ± 2.8 in *nlrp3*$^{+/+}$ and 31.8 ± 2.1 in *nlrp3*$^{-/-}$ mice) with increased CSA (0.49 ± 0.04 μm^2 and 0.50 ± 0.04 μm^2 in *nlrp3*$^{+/+}$ and *nlrp3*$^{-/-}$ mice, respectively, Suppl. Fig. 2G and H), which were completely compacted with intact well-organized cristae. Intermyofibrillar distribution of the sarcoplasmic reticulum

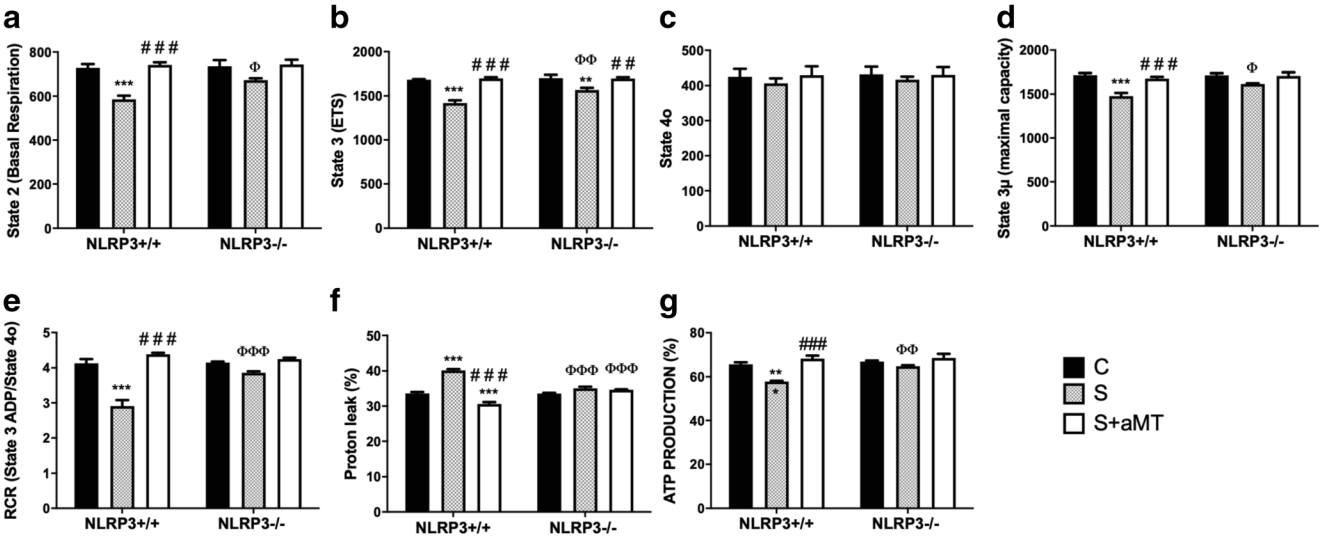

Fig. 3 Changes in mitochondrial respiration. Experiments were performed in heart of control and septic *nlrp3*$^{+/+}$ and *nlrp3*$^{-/-}$ mice, with or without melatonin treatment. **a** Changes in basal respiration (State 2). **b** Phosphorylating respiration (State 3, in the presence of ADP and substrate). **c** Resting respiration (State 4o, with the addition of oligomycin). **d** Maximal uncoupler-stimulated respiration (State 3μ, with the addition of FCCP). **e** Respiratory control ratios (RCR; State 3/State 4o). **f** Proton leak. **g** ATP production. Data are expressed as mean ± SEM of $n = 6$ animals/group. C, control; S, sepsis; and S+aMT, septic animals treated with 3 × 30 mg/kg melatonin. $^{**}p < 0.01$ and $^{***}p < 0.001$ *v.* C; $^{\#\#}p < 0.01$, $^{\#\#\#}p < 0.001$ *v.* S; $^{\Phi}p < 0.05$, $^{\Phi\Phi}p < 0.01$, and $^{\Phi\Phi\Phi}p < 0.001$, *v. nlrp3*$^{+/+}$

and little interstitial tissues were observed in addition to the presence of lipid droplets (L) (Suppl. Fig. 2C and F).

The absence of NLRP3 reduces the apoptotic response to sepsis in the heart of mice, which is prevented by melatonin

A reduced oxidative stress in *nlpr3*$^{-/-}$ mice should be reflected in a reduction in mitochondrial damage and subsequent reduction in apoptotic events. To address this question, we analyzed the cell death signals in response to sepsis. *nlrp3*$^{+/+}$ animals increased Bax/Bcl2 protein and mRNA ratio during sepsis, an event related to the release of apoptotic signals from the mitochondria to the cytosol. These changes paralleled a rise in the protein content and mRNA expression of these apoptotic markers (Fig. 4a and b). Mice lacking NLRP3, however, showed a lower increase in Bax/Bcl2 ratio during sepsis compared with *nlrp3*$^{+/+}$ mice. Melatonin maintained the Bax/Bcl2 ratio at control levels in *nlrp3*$^{+/+}$ and *nlpr3*$^{-/-}$ mice, an effect reflecting the reduction in Bax and enhanced Bcl2 expression and protein content.

To further analyze the anti-apoptotic role of melatonin, we measured the p53 turnover and caspase-3 and caspase-9 expression in these mice. Our results showed that the accumulation of p53 in the nucleus during sepsis was higher in *nlrp3*$^{+/+}$ than in *nlpr3*$^{-/-}$ mice, paralleling the changes in Bax/Bcl2 ratio (Fig. 5a). These findings were supported by the increased *p53* mRNA expression in *nlrp3*$^{+/+}$ but not in *nlpr3*$^{-/-}$ mice. Caspase-9 and caspase-3 expression rose in *nlrp3*$^{+/+}$ but not in mutant mice during sepsis (Fig. 5b). Equivalent changes were identified in the protein content of cleaved caspase-3, giving an apoptotic index significantly elevated in *nlrp3*$^{+/+}$ during sepsis, which remained at control levels in *nlpr3*$^{-/-}$ septic mice (Fig. 5c). The low apoptotic response to sepsis in mice lacking NLRP3 compared with *nlrp3*$^{+/+}$ mice may depend on the maintenance of a significant HO-1 response to Nrf2 and a lower oxidative stress state in the former (Fig. 2). In all cases, melatonin administration counteracted the effects of sepsis, restoring the control values of these apoptotic markers.

To confirm these data, fluorescence analysis of myocardial tissue following Hoechst staining was done. Compared with control *nlrp3*$^{+/+}$ mice (Suppl. Fig. 3A), sepsis induced a significant rise in the number of apoptotic cells during sepsis (Suppl. Fig. 3B), which was counteracted by

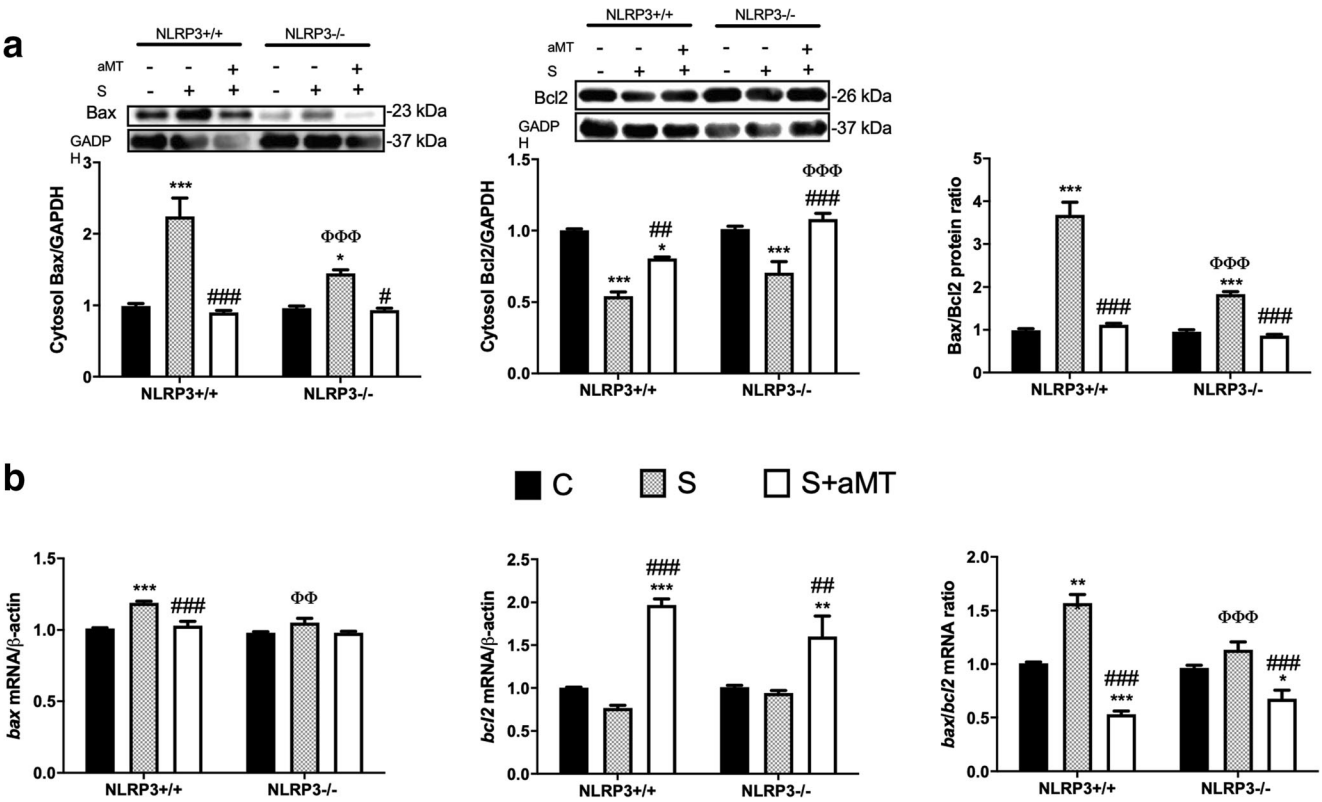

Fig. 4 Changes in Bax and Bcl2 turnover during sepsis. Experiments were performed in hearts of control and septic *nlrp3*$^{+/+}$ and *nlrp3*$^{-/-}$ mice, with or without melatonin treatment. Analysis of mRNA expression (qRT-PCR) and cytosolic and nuclear protein content (western blot) in mice. **a** Cytosolic protein levels of Bax and Bcl2, and Bax/Bcl2 ratio. **b** mRNA expression of *bax* and *bcl2*, and *bax/bcl-2* ratio. Data are expressed as mean ± SEM of $n = 6$ animals/group. C, control; S, sepsis; S+aMT, septic animals treated with 3 × 30 mg/kg melatonin. $^{*}p < 0.05$, $^{**}p < 0.01$, and $^{***}p < 0.001$ *v.* C; $^{\#}p < 0.05$, $^{\#\#}p < 0.01$, and $^{\#\#\#}p < 0.001$ *v.* S; $^{\Phi\Phi}p < 0.01$ and $^{\Phi\Phi\Phi}p < 0.001$ *v. nlrp3*$^{+/+}$

melatonin treatment (Suppl. Fig. 3C). Apoptotic cells showed the typical blebbing, cell shrinkage, nuclear fragmentation, chromatin condensation, and chromosomal DNA fragmentation. Control *nlrp3*$^{-/-}$ cardiomyocytes showed less apoptosis than these cells in *nlrp3*$^{+/+}$ mice (Suppl. Fig. 3D); sepsis also produced fewer fragmented nuclei (20%) than in *nlrp3*$^{+/+}$ (50%) (Suppl. Fig. 3E). Melatonin clearly counteracted these changes in apoptosis, supporting the reported alterations in the apoptotic markers (Suppl. Fig. 3F).

The absence of NLRP3 or melatonin treatment reduce autophagy and mitophagy events during sepsis in the heart of mice

An oxidative environment results in mitochondrial dysfunction and also autophagy/mitophagy. Various molecular pathways are involved in ROS-dependent autophagy; these include ROS-LC3, ROS-Nrf2-p62, and ROS-HIF1-Nix (Li et al. 2015), and they are depicted in Fig. 6. Sepsis induced an increase in LC3-II/LC3-I ratio, p62 content, HIF1, and Nix

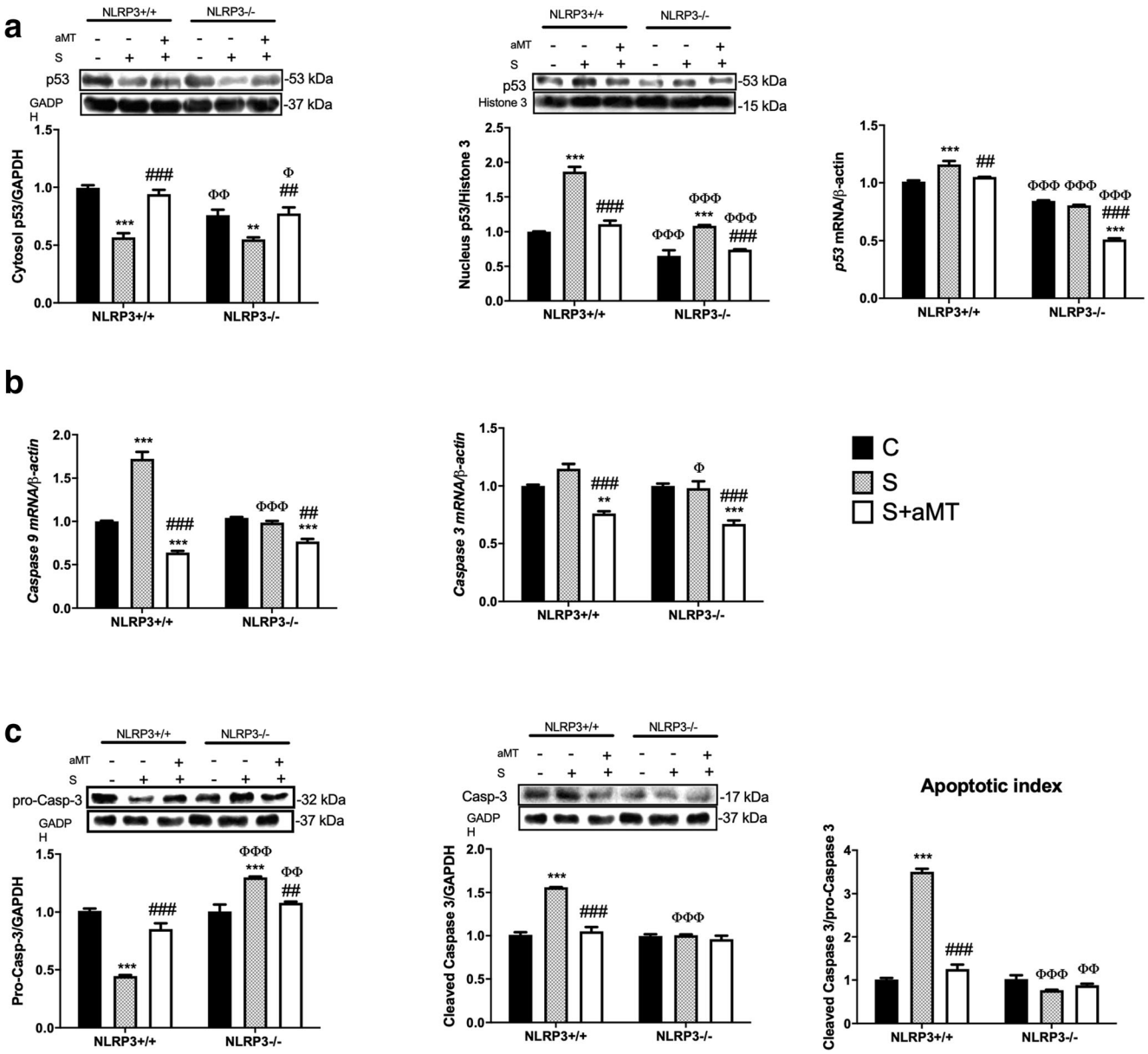

Fig. 5 Changes in p53 and caspases during sepsis. Experiments were performed in hearts of control and septic *nlrp3*$^{+/+}$ and *nlrp3*$^{-/-}$ mice, with or without melatonin treatment. **a** Cytosolic and nuclear p53 protein content and *p53* mRNA levels. **b** mRNA levels of *caspase-3* and *caspase-9*. **c** Cytosolic cleaved caspase-3 and pro-caspase-3 protein content, and the cleaved caspase-3/pro-caspase-3 ratio, as apoptotic index. Data are expressed as mean ± SEM of $n = 6$ animals/group. C, control; S, sepsis; S+aMT, septic animals treated with 3 × 30 mg/kg melatonin. $^{**}p < 0.01$ and $^{***}p < 0.001$ *v.* C; $^{\#\#}p < 0.01$ and $^{\#\#\#}p < 0.001$ *v.* S; $^{\Phi}p < 0.05$, $^{\Phi\Phi}p < 0.01$, and $^{\Phi\Phi\Phi}p < 0.001$ *v. nlrp3*$^{+/+}$

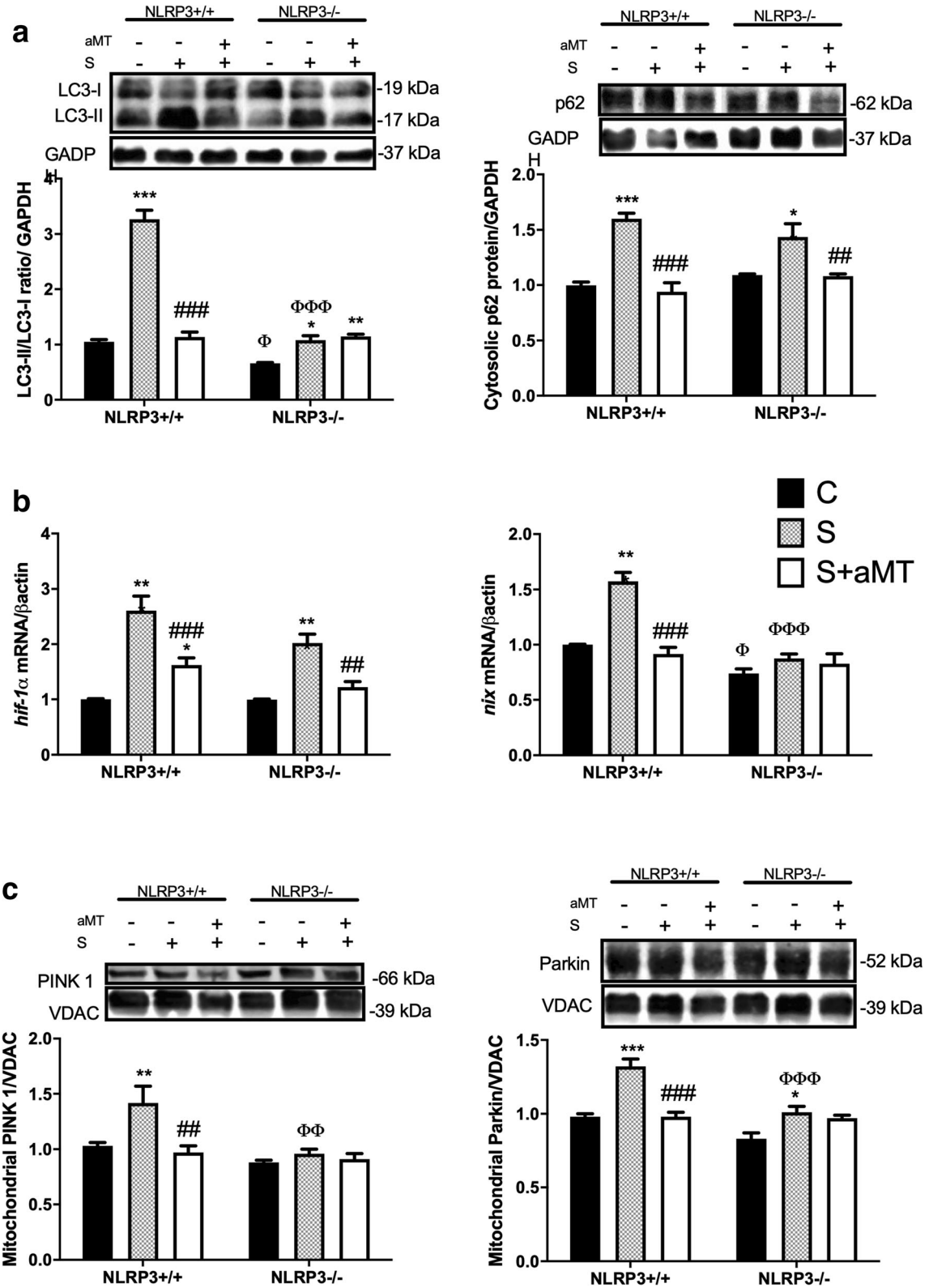

Fig. 6 Melatonin and NLRP3 deficiency reduced autophagy/mitophagy events in septic mice. Experiments were performed in hearts of control and septic *nlrp3*$^{+/+}$ and *nlrp3*$^{-/-}$ mice, with or without melatonin treatment. **a** LC3II/I ratio and cytosolic p62 protein content. **b** mRNA levels of *hif-1*α and *nix*. **c** mitochondrial PINK1 and Parkin protein content. Data are expressed as mean ± SEM of $n = 6$ animals/group. C, control; S, sepsis; S+aMT, septic animals treated with 3 × 30 mg/kg melatonin. $^{*}p < 0.05$, $^{**}p < 0.01$, and $^{***}p < 0.001$ *v.* C; $^{\#\#}p < 0.01$ and $^{\#\#\#}p < 0.001$ *v.* S; $^{\Phi}p < 0.05$, $^{\Phi\Phi}p < 0.01$, and $^{\Phi\Phi\Phi}p < 0.001$ *v. nlrp3*$^{+/+}$

in *nlrp3*$^{+/+}$ mice (Fig. 6a and b), supporting the presence of autophagy in septic mice. The absence of NLRP3 inflammasome reduced these responses except for p62 and HIF1, suggesting that melatonin treatment blunted autophagy. PINK1 and Parkin, two markers of mitophagy, also increased in *nlrp3*$^{+/+}$ mice during sepsis, and they were almost blocked in *nlrp3*$^{-/-}$ mice. Also, melatonin treatment reduced totally the induction of PINK1 and Parkin (Fig. 6c).

The absence of NLRP3 or melatonin treatment modify mitochondrial dynamics during sepsis in the heart of mice

Mitochondrial fission precedes mitophagy and, so, we measured the content of Drp1 and Mfn2 during sepsis to analyze changes in mitochondrial fission/fusion. Sepsis increases the content of Drp1 in *nlrp3*$^{+/+}$ mice, with a parallel reduction in Mfn2, suggesting the prevalence of fission events in septic mice (Fig. 7a). These changes were less marked in *nlrp3*$^{-/-}$ mice. Melatonin administration or the absence of NLRP3 inflammasome prevented the increase of Drp1, maintaining the levels of Mfn2, increasing the ratio Mfn2/Drp1 (Fig. 7b). These data support the predominance of fusion events, preventing mitophagy.

Discussion

It was suggested that, due to either the reduction of oxidative stress or through a direct interaction between the Nrf2/Keap1 and NLRP3 complexes, Nrf2 activation may inhibit NLRP3 inflammasome activation during inflammation (Garstkiewicz et al. 2017; Liu et al. 2017). Our study provides important new information related to Nrf2/NLRP3 connection. First, Nrf2 turnover was similar in *nlrp3*$^{+/+}$ and *nlrp3*$^{-/-}$ mice during sepsis, which means that the regulation of the former was independent of the NLRP3 inflammasome activation. Second, collected data support the reduction of apoptosis and mitophagy in the absence of NLRP3 inflammasome activation, which reflect a lower ROS production and better mitochondrial function in *nlrp3*$^{-/-}$ than in *nlrp3*$^{+/+}$ mice during sepsis. Third, melatonin treatment further enhanced Nrf2 translocation to the nucleus and increased *ho-1* expression in both mouse strains, modulating the antioxidant response to sepsis. In general, melatonin counteracted the effects of sepsis in *nlrp3*$^{+/+}$ mice with minor effects in mutant mice. The results reflect the parallelism between melatonin effects and absence of NLRP3 inflammasome activation (Rahim et al. 2017), which may account not only for the control of Nrf2 response by melatonin but also for the capacity of melatonin to inhibit the NLRP3 inflammasome activation in sepsis recently reported (Garcia et al. 2015; Volt et al. 2016). Thus, the melatonin/Nrf2 connection may collaborate in the redox and mitochondrial homeostasis, preventing myocardial failure during sepsis.

The immune response during sepsis depends on the activation of the NF-κB pathway, its induction of oxidative stress and mitochondrial dysfunction, and the subsequent triggering of the NLRP3 inflammasome (Garcia et al. 2015). NF-κB-derived pro-oxidants and the antioxidant Nrf2 are co-released during inflammation; the latter becomes an essential response in an attempt to reduce the excess ROS, mitochondrial damage, and the NLRP3 inflammasome activation (Garstkiewicz et al. 2017; Liu et al. 2017; Vilhardt et al. 2017). It was reported by us that the lack of the NLRP3 inflammasome in *nlrp3*$^{-/-}$ mice converts sepsis to a moderate inflammatory disease with a reduction in the myocardial impairment during sepsis (Martin et al. 2000; Gustafsson and Gottlieb 2003; Kensler et al. 2007; Abdullah et al. 2012). Thus, this model may yield further information regarding the Nrf2/NLRP3 inflammasome connection in sepsis.

Nrf2 is a pivotal bZIP transcription factor that maintains intracellular redox homeostasis by regulating a series of

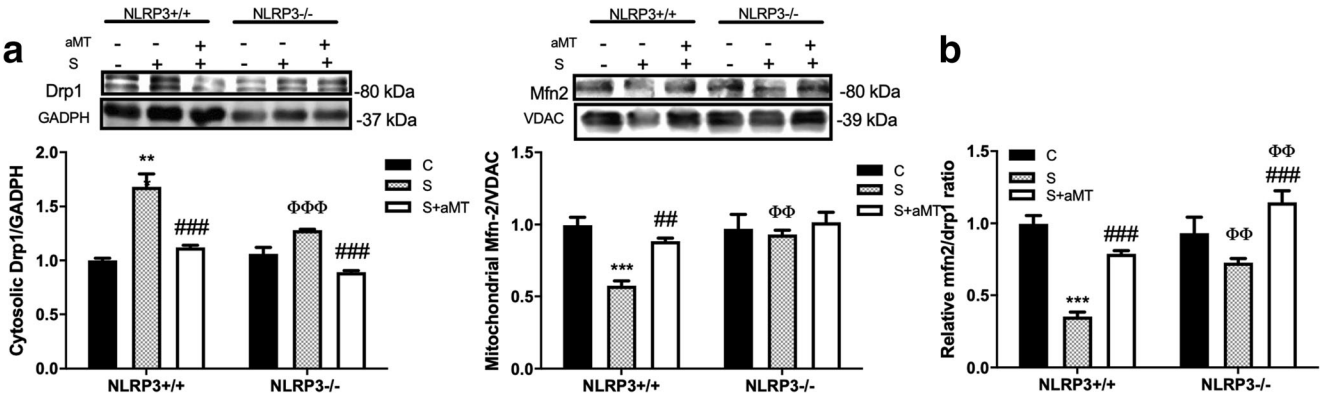

Fig. 7 Changes in mitochondrial fission/fusion during sepsis after melatonin treatment and NLRP3 deficiency. Experiments were performed in hearts of control and septic *nlrp3*$^{+/+}$ and *nlrp3*$^{-/-}$ mice, with or without melatonin treatment. **a** Cytosolic Drp1 and mitochondrial Mfn2 protein content. **b** Mfn2/Drp1 ratio. Data are expressed as mean ± SEM of $n = 6$ animals/group. C, control; S, sepsis; S+aMT, septic animals treated with 3 × 30 mg//kg melatonin. $^{***}p < 0.001$ *v.* C; $^{\#\#}p < 0.01$ and $^{\#\#\#}p < 0.001$ *v.* S; $^{\Phi\Phi}p < 0.01$ and $^{\Phi\Phi\Phi}p < 0.001$ *v. nlrp3*$^{+/+}$

cytoprotective genes in response to diverse stimuli, including LPS and ROS (Kensler et al. 2007; Loboda et al. 2016). Under basal conditions, Nrf2 is sequestered by Keap1 in the cytoplasm (Itoh et al. 1999; Zhang et al. 2004), leading to its subsequent proteasomal degradation. In response to oxidative stress, ROS modify the critical cysteine thiols of Keap1, resulting in a conformational change of Keap1 and a reduction of Nrf2 degradation; this allows Nrf2 phosphorylation by protein kinase C at conserved site Serine-40 (or Ser40) and possibly other kinases such as PI3K/Akt. The events enable pSer40 Nrf2 nuclear accumulation and transactivation of antioxidant response element (ARE)-dependent genes involved in oxidative and xenobiotic stress responses and in the induction of mitochondrial biogenesis (Bloom and Jaiswal 2003; Magesh et al. 2012).

The first finding of interest reported here is the reduction of cytosolic Keap1 protein allowing the Nrf2 increase (Bloom and Jaiswal 2003; Magesh et al. 2012). Although a close relationship between Nrf2 and the NLRP3 inflammasome has been reported (Garstkiewicz et al. 2017), we show here that the presence or absence of NLRP3 inflammasome did not interfere with Nrf2 expression and the nuclear accumulation of its active form, pSer40 Nrf2. Moreover, although the protective role of Nrf2 in multiple inflammatory diseases has been reported (Thimmulappa et al. 2006; Kong et al. 2011), it does not occur in sepsis. Even with enhanced expression of *ho-1*, which has anti-apoptotic, antioxidant, and anti-inflammatory activities (Loboda et al. 2016), Nrf2 activation is insufficient to counteract the inflammation and subsequent oxidative stress, which induced mitochondrial damage and NLRP3 inflammasome activation. Nevertheless, mice lacking NLRP3 had lower antioxidant response than wild-type ones, suggesting less oxidative damage that depends on the lack of the inflammasome and not of Nrf2 activation.

The fact that *ho-1* expression was induced to a similar extent in $nlrp3^{+/+}$ and $nlrp3^{-/-}$ mice during sepsis suggests that Nrf2 is functional in both of them. Our results also show an enhanced expression and activity of SOD and GPx in $nlrp3^{+/+}$ but not in $nlrp3^{-/-}$ mice during sepsis. GPx consumes GSH, a major determinant of the redox defense (Go and Jones 2008), and the GSSG produced is recycled to GSH via GRd (Dickinson and Forman 2002). The inhibition of GRd expression and activity here found reduces the efficacy of the GSH cycle, favoring an oxidative environment (Acuña-Castroviejo et al. 2011; Garcia et al. 2015; Volt et al. 2016).

In addition to NF-κB and NLRP3 inflammasome, excessive ROS can modify the mitochondrial membrane potential and induce the release of cytochrome c into the cytosol, eventually leading to apoptosis of cardiomyocytes (Kaltschmidt et al. 2000; Gustafsson and Gottlieb 2003). Here, we found a significant reduction in mitochondrial function, including reduced RCR and ATP production, with increased proton leak in $nlrp3^{+/+}$ mice, but not in mutant mice. These changes parallel the structural modifications of myocardial mitochondria in $nlrp3^{+/+}$ compared with $nlrp3^{-/-}$ mice during sepsis. Besides mitochondrial protection against oxidative damage (Sun et al. 2015), Nrf2 may exert a direct regulation of mitochondrial function. These data are based on studies with *nrf2*-deficient or Nrf2-primed mice (Abdullah et al. 2012; Holmstrom et al. 2013). We show here, however, that the sole activation of Nrf2 in wild-type mice during sepsis is unable to prevent mitochondrial damage and subsequent events including apoptosis. Even more, our findings agree with studies in $nlrp3^{-/-}$ mice, which exhibit alleviation in non-septic models of disease (Sandanger et al. 2013; Zhuang et al. 2014), and further support the essential role of the inflammasome in sepsis. However, whether the regulation of apoptosis is mediated by NLRP3 inflammasome is yet unclear (Wheeler 2011).

It was suggested that autophagy has a protective role during sepsis, event reducing apoptosis that, in turn, may inhibit autophagy (Marino et al. 2014; Mukhopadhyay et al. 2014; Feng et al. 2019). Three main pathways underlie autophagy regulated by ROS, including ROS-LC3, ROS-Nrf2-p62, and ROS-HIF-1-Nix (Li et al. 2015). Here, we found that these pathways were activated during sepsis in $nlrp3^{+/+}$ mice, with almost no activation in mutant mice. The coexistence of apoptosis and autophagy may be explained because autophagy may disrupt components of the cell leading to apoptosis. This occurs in our experimental model where autophagy and apoptosis run together in wild-type mice. Mutant mice, however, were more resistant to autophagy and apoptosis, revealing again that the inflammation driven by the NLRP3 inflammasome activation during sepsis is a key component of these responses. In parallel, we detected also an enhanced PINK1 and Parkin-mediated mitophagy, which may attempt to reduce NLRP3 inflammasome activation (Lin et al. 2019). The activation of Drp1 and reduction of Mfn2 during sepsis in wild-type mice, but not in mutant mice, account for the presence of mitophagy. These circumstances downgrade the activation of NLRP3 inflammasome that may modulate the septic response (Lin et al. 2019). But this does not occur in our experimental model of sepsis, because septic mice die without treatment; only NLRP3-deficient mice are resistant and they survive to sepsis. Collectively, these data explain that in severe sepsis, all mechanisms including autophagy, mitophagy, and apoptosis are launched in a disorganized way.

We have no definitive pharmacological tools for sepsis treatment. Experimental sepsis and clinical data show that melatonin behaves as an outstanding anti-inflammatory and antioxidant molecule with demonstrated efficacy to counteract the NF-κB/NLRP3 inflammasome activation during sepsis in cardiomyocytes (Gitto et al. 2001; Escames et al. 2007; Ortiz et al. 2014; Garcia et al. 2015; Volt et al. 2016; Rahim et al. 2017). We analyzed here whether these effects of melatonin are mediated through the Nrf2 pathway. It is known that melatonin exerts a regulatory role on the Keap1-Nrf2 system (Vriend and Reiter 2015), and the indolamine exerts beneficial

effects on multiple experimental conditions including sepsis by activating the Nrf2 pathway through Sirt1, AMPK, and other signaling pathways (Arioz et al. 2019; Li et al. 2019b; Wang et al. 2019).

Melatonin administration further upregulated Nrf2 expression and protein levels in both septic mouse strains to the same extent, in parallel with the reduction of inflammatory mediators. The effects of melatonin depend on the increased expression of Nrf2 because Keap1 was unmodified by the indolamine. As a result, melatonin enhanced *ho-1* expression, potentiating its protective effects, modulating the antioxidative response. Together with the inhibition of the NF-κB/NLRP3 inflammasome connection, melatonin also reduces the redox response due to its direct ROS scavenging activity report (Acuña Castroviejo et al. 2017; Reiter et al. 2017). In *nlrp3*$^{-/-}$ mice, melatonin, however, stimulated SOD, and GRd expression and activity but not CAT, without changing the expression of *gpx*. Thus, it seems that melatonin maintains a minimal antioxidant capacity in mutant mice during sepsis, sufficient to promote a further reduction in the oxidative stress level. These marked capabilities of melatonin prevented mitochondrial dysfunction controlling autophagy/mitophagy/apoptosis. Interestingly, the effects of melatonin to reduce the pathophysiological environment in wild-type septic mice were similar to those obtained by the elimination of *nlrp3* gene, although melatonin in *nlrp3*$^{-/-}$ mice further reduced the small damage due to sepsis. Moreover, the known mitochondrial protective effects of melatonin (Martin et al. 2000; Escames et al. 2003, 2007; Acuña-Castroviejo et al. 2011; Volt et al. 2016; Acuña Castroviejo et al. 2017) were here also observed. Melatonin improved mitochondrial bioenergetics by preserving ETC activity and the proton gradient required for ATP synthesis, reducing autophagy/mitophagy/apoptosis during sepsis. An interesting observation is that the apoptotic process was similarly reduced during sepsis in *nlrp3*$^{+/+}$ mice by melatonin treatment and in untreated *nlrp3*$^{-/-}$ mice in the absence of NLRP3. The anti-apoptotic effects of melatonin described here may be related to Nrf2 activation, HO-1 induction, and the inhibition of the PINK1/Parkin and the NF-κB/NLRP3 network effects that were reported in other experimental conditions (Garcia et al. 2015; Diaz-Casado et al. 2016; Shi et al. 2019).

Our study suggests that melatonin seems to exert its therapeutic effect, in part, via Nrf2/HO-1 signaling pathway activation during sepsis, significantly reducing myocardial damage by enhancing Nrf2 signaling to reduce NLRP3 inflammasome and mitochondrial damage, thereby preventing apoptosis. It is evident that Nrf2 activation during sepsis is unable to prevent the course of sepsis but further enhancing its induction by melatonin promotes a response enough to reduce sepsis severity. Thus, melatonin becomes a type of molecule to have in mind for its therapeutic use.

Conclusion

Our studies suggest that melatonin reduced myocardial damage during sepsis by enhancing Nrf2 signaling to reduce NLRP3 inflammasome and mitochondrial oxidative damage and thereby preventing apoptosis. Thus, melatonin seems to exert its therapeutic effect, in part, via Nrf2/HO-1 signaling pathway activation during sepsis.

Author contributions I.R and D.A.-C designed the study, and reviewed and edited the manuscript; R.K.S, M.F-O., and P.A.-M performed the experiments; A.G.-L, J.F.-M., and I.R. analyzed the data; GE and BD drafted the manuscript. All data included in the manuscript were generated in-house and no paper mill was used.

Funding This study was partially supported by grants from the Instituto de Salud Carlos III (Ministerio de Economía y Competitividad, Spain, through the projects, PI16-00519 and CB16-10-00238 (Co-funded by European Regional Development Fund/European Social Fund) "Investing in your future") and from the Consejería de Innovación, Ciencia y Empresa, Junta de Andalucía (P10-CTS-5784, and CTS-101), Spain. M F-O is supported by a FPU fellowship from the Ministerio de Educación, Spain.

Data availability The datasets generated and analyzed during the current study are available from the corresponding author on reasonable request.

Compliance with ethical standards

Conflict of interest The authors declare that they have no conflict of interest.

Ethics approval This study was performed in accordance with the National Institutes of Health Guide for the Care and Use of Laboratory Animals (National Research Council, National Academy of Sciences, Bethesda, MD, USA), the European Convention for the Protection of Vertebrate Animals used for Experimental and Other Scientific Purposes (CETS # 123), and the Spanish law for animal experimentation (R.D. 53/2013). The final study was approved by Andalusian's Ethical Committee (protocol number: 462-CEEA-2013) (Spain).

Consent to participate All authors gave their consent to participate in this study.

Consent for publication All authors gave their consent for the publication of this manuscript.

Code availability Not applicable.

References

Abdullah A, Kitteringham NR, Jenkins RE, Goldring C, Higgins L, Yamamoto M, Hayes J, Park BK (2012) Analysis of the role of Nrf2 in the expression of liver proteins in mice using two-dimensional gel-based proteomics. Pharmacol Rep 64:680–697. https://doi.org/10.1016/s1734-1140(12)70863-0

Acuña Castroviejo D, Rahim I, Acuña-Fernández C, Fernández-Ortiz M, Solera-Martín J, Sayed RKA, Díaz-Casado ME, Rusanova I, López LC, Escames G (2017) Melatonin, clock genes and mitochondria in

sepsis. Cell Mol Life Sci 74:3965–3987. https://doi.org/10.1007/s00018-017-2610-1

Acuña-Castroviejo D, López LC, Escames G, López A, García JA, Reiter RJ (2011) Melatonin-mitochondria interplay in health and disease. Curr Top Med Chem 11:221–240. https://doi.org/10.2174/156802611794863517

Aebi H (1984) Catalase in vitro. Methods Enzymol 105:121–126. https://doi.org/10.1016/S0076-6879(84)05016-3

Ahmed SM, Luo L, Namani A, Wang XJ, Tang X (2017) Nrf2 signaling pathway: pivotal roles in inflammation. Biochim Biophys Acta Mol basis Dis 1863:585–597. https://doi.org/10.1016/j.bbadis.2016.11.005

Alvarez S, Vico T, Vanasco V (2016) Cardiac dysfunction, mitochondrial architecture, energy production, and inflammatory pathways: interrelated aspects in endotoxemia and sepsis. Int J Biochem Cell Biol 81:307–314. https://doi.org/10.1016/j.biocel.2016.07.032

Arioz BI, Tastan B, Tarakcioglu E, Tufekci KU, Olcum M, Ersoy N, Bagriyanik A, Genc K, Genc S (2019) Melatonin attenuates LPS-induced acute depressive-like behaviors and microglial NLRP3 Inflammasome activation through the SIRT1/Nrf2 pathway. Front Immunol 10:1511. https://doi.org/10.3389/fimmu.2019.01511

Bloom DA, Jaiswal AK (2003) Phosphorylation of Nrf2 at Ser40 by protein kinase C in response to antioxidants leads to the release of Nrf2 from INrf2, but is not required for Nrf2 stabilization/accumulation in the nucleus and transcriptional activation of antioxidant response element-mediated NAD(P)H:quinone oxidoreductase-1 gene expression. J Biol Chem 278:44675–44682. https://doi.org/10.1074/jbc.M307633200

Bradford MM (1976) A rapid and sensitive method for the quantitation of microgram quantities of protein utilizing the principle of protein-dye binding. Anal Biochem 72:248–254. https://doi.org/10.1016/0003-2697(76)90527-3

Crespo E, Macias M, Pozo D, Escames G, Martin M, Vives F, Guerrero JM, Acuña-Castroviejo D (1999) Melatonin inhibits expression of the inducible NO synthase II in liver and lung and prevents endotoxemia in lipopolysaccharide-induced multiple organ dysfunction syndrome in rats. FASEB J 13:1537–1546. https://doi.org/10.1096/fasebj.13.12.1537

Diaz-Casado ME, Lima E, Garcia JA, Doerrier C, Aranda P, Sayed RK, Guerra-Librero A, Escames G, Lopez LC, Acuna-Castroviejo D (2016) Melatonin rescues zebrafish embryos from the parkinsonian phenotype restoring the parkin/PINK1/DJ-1/MUL1 network. J Pineal Res 61:96–107. https://doi.org/10.1111/jpi.12332

Dickinson DA, Forman HJ (2002) Glutathione in defense and signaling: lessons from a small thiol. Ann N Y Acad Sci 973:488–504. https://doi.org/10.1111/j.1749-6632.2002.tb04690.x

Dimauro I, Pearson T, Caporossi D, Jackson MJ (2012) A simple protocol for the subcellular fractionation of skeletal muscle cells and tissue. BMC Res Notes 5:513. https://doi.org/10.1186/1756-0500-5-513

Doerrier C, Garcia JA, Volt H, Diaz-Casado ME, Luna-Sanchez M, Fernandez-Gil B, Escames G, Lopez LC, Acuña-Castroviejo D (2016) Permeabilized myocardial fibers as model to detect mitochondrial dysfunction during sepsis and melatonin effects without disruption of mitochondrial network. Mitochondrion 27:56–63. https://doi.org/10.1016/j.mito.2015.12.010

Escames G, Leon J, Macias M, Khaldy H, Acuña-Castroviejo D (2003) Melatonin counteracts lipopolysaccharide-induced expression and activity of mitochondrial nitric oxide synthase in rats. FASEB J 17:932–934. https://doi.org/10.1096/fj.02-0692fje

Escames G, López LC, Ortiz F, López A, García JA, Ros E, Acuña-Castroviejo D (2007) Attenuation of cardiac mitochondrial dysfunction by melatonin in septic mice. FEBS J 274:2135–2147. https://doi.org/10.1111/j.1742-4658.2007.05755.x

Feng Y, Liu B, Zheng X, Chen L, Chen W, Fang Z (2019) The protective role of autophagy in sepsis. Microb Pathog 131:106–111. https://doi.org/10.1016/j.micpath.2019.03.039

Gallego-Selels A, Martin-Rincon M, Martinez-Canton M, Perez-Valera M, Martin-Rodriguez S, Gelabert-Rebato M, Santana A, Morales-Alamo D, Dorado C, Calbet JAL (2020) Regulation of Nrf2/Keap1 signalling in human skeletal muscle during exercise to exhaustion in normoxia, severe acute hypoxia and post-exercise ischaemia: Influence of metabolite accumulation and oxygenation. Redox Biol 36. https://doi.org/10.1016/j.redox.2020.101627

Garcia JA, Volt H, Venegas C, Doerrier C, Escames G, Lopez LC, Acuña-Castroviejo D (2015) Disruption of the NF-kappaB/NLRP3 connection by melatonin requires retinoid-related orphan receptor-alpha and blocks the septic response in mice. FASEB J 29:3863–3875. https://doi.org/10.1096/fj.15-273656

Garstkiewicz M, Strittmatter GE, Grossi S, Sand J, Fenini G, Werner S, French LE, Beer HD (2017) Opposing effects of Nrf2 and Nrf2-activating compounds on the NLRP3 inflammasome independent of Nrf2-mediated gene expression. Eur J Immunol 47:806–817. https://doi.org/10.1002/eji.201646665

Gitto E, Karbownik M, Reiter RJ, Tan DX, Cuzzocrea S, Chiurazzi P, Cordaro S, Corona G, Trimarchi G, Barberi I (2001) Effects of melatonin treatment in septic newborns. Pediatr Res 50:756–760. https://doi.org/10.1203/00006450-200112000-00021

Go YM, Jones DP (2008) Redox compartmentalization in eukaryotic cells. Biochim Biophys Acta 1780:1273–1290. https://doi.org/10.1016/j.bbagen.2008.01.011

Gustafsson AB, Gottlieb RA (2003) Mechanisms of apoptosis in the heart. J Clin Immunol 23:447–459. https://doi.org/10.1023/B:JOCI.0000010421.56035.60

Holmstrom KM, Baird L, Zhang Y, Hargreaves I, Chalasani A, Land JM, Stanyer L, Yamamoto M, Dinkova-Kostova AT, Abramov AY (2013) Nrf2 impacts cellular bioenergetics by controlling substrate availability for mitochondrial respiration. Biol Open 2:761–770. https://doi.org/10.1242/bio.20134853

Huang J, Philbert MA (1996) Cellular responses of cultured cerebellar astrocytes to ethacrynic acid-induced perturbation of subcellular glutathione homeostasis. Brain Res 711:184–192. https://doi.org/10.1016/0006-8993(95)01376-8

Hunter JD, Doddi M (2010) Sepsis and the heart. Br J Anaesth 104:3–11. https://doi.org/10.1093/bja/aep339

Itoh K, Wakabayashi N, Katoh Y, Ishii T, Igarashi K, Engel JD, Yamamoto M (1999) Keap1 represses nuclear activation of antioxidant responsive elements by Nrf2 through binding to the amino-terminal Neh2 domain. Genes Dev 13:76–86. https://doi.org/10.1101/gad.13.1.76

Jaskot RH, Charlet EG, Grose EC, Grady MA, Roycroft JH (1983) An automated analysis of glutathione peroxidase, S-transferase, and reductase activity in animal tissue. J Anal Toxicol 7:86–88. https://doi.org/10.1093/jat/7.2.86

Kaltschmidt B, Kaltschmidt C, Hofmann TG, Hehner SP, Droge W, Schmitz ML (2000) The pro- or anti-apoptotic function of NF-kappaB is determined by the nature of the apoptotic stimulus. Eur J Biochem 267:3828–3835. https://doi.org/10.1046/j.1432-1327.2000.01421.x

Kensler TW, Wakabayashi N, Biswal S (2007) Cell survival responses to environmental stresses via the Keap1-Nrf2-ARE pathway. Annu Rev Pharmacol Toxicol 47:89–116. https://doi.org/10.1146/annurev.pharmtox.46.120604.141046

Kong X, Thimmulappa R, Craciun F, Harvey C, Singh A, Kombairaju P, Reddy SP, Remick D, Biswal S (2011) Enhancing Nrf2 pathway by disruption of Keap1 in myeloid leukocytes protects against sepsis. Am J Respir Crit Care Med 184:928–938. https://doi.org/10.1164/rccm.201102-0271OC

Lambertucci F, Motino O, Villar S, Rigalli JP, de Lujan AM, Catania VA, Martin-Sanz P, Carnovale CE, Quiroga AD, Frances DE, Ronco

MT (2017) Benznidazole, the trypanocidal drug used for Chagas disease, induces hepatic NRF2 activation and attenuates the inflammatory response in a murine model of sepsis. Toxicol Appl Pharmacol 315:12–22. https://doi.org/10.1016/j.taap.2016.11.015

Latt SA, Stetten G, Juergens LA, Willard HF, Scher CD (1975) Recent developments in the detection of deoxyribonucleic acid synthesis by 33258 Hoechst fluorescence. J Histochem Cytochem 23:493–505. https://doi.org/10.1177/23.7.1095650

Latz E, Xiao TS, Stutz A (2013) Activation and regulation of the inflammasomes. Nat Rev Immunol 13:397–411. https://doi.org/10.1038/nri3452

Li L, Tan J, Miao Y, Lei P, Zhang Q (2015) ROS and Autophagy: interactions and molecular regulatory mechanisms. Cell Mol Neurobiol 35:615–621. https://doi.org/10.1007/s10571-015-0166-x

Li N, Zhou H, Wu H, Wu Q, Duan M, Deng W, Tang Q (2019a) STING-IRF3 contributes to lipopolysaccharide-induced cardiac dysfunction, inflammation, apoptosis and pyroptosis by activating NLRP3. Redox Biol 24:101215. https://doi.org/10.1016/j.redox.2019.101215

Li J, Zheng X, Ma X, Xu X, Du Y, Lv Q, Li X, Wu Y, Sun H, Yu L, Zhang Z (2019b) Melatonin protects against chromium(VI)-induced cardiac injury via activating the AMPK/Nrf2 pathway. J Inorg Biochem 197:110698. https://doi.org/10.1016/j.jinorgbio.2019.110698

Lin Q, Li S, Jiang N, Shao X, Zhang M, Jin H, Zhang Z, Shen J, Zhou Y, Zhou W, Gu L, Lu R, Ni Z (2019) PINK1-parkin pathway of mitophagy protects against contrast-induced acute kidney injury via decreasing mitochondrial ROS and NLRP3 inflammasome activation. Redox Biol 26:101254. https://doi.org/10.1016/j.redox.2019.101254

Liu X, Zhang X, Ding Y, Zhou W, Tao L, Lu P, Wang Y, Hu R (2017) Nuclear factor E2-related factor-2 negatively regulates NLRP3 inflammasome activity by inhibiting reactive oxygen species-induced NLRP3 priming. Antioxid Redox Signal 26:28–43. https://doi.org/10.1089/ars.2015.6615

Loboda A, Damulewicz M, Pyza E, Jozkowicz A, Dulak J (2016) Role of Nrf2/HO-1 system in development, oxidative stress response and diseases: an evolutionarily conserved mechanism. Cell Mol Life Sci 73:3221–3247. https://doi.org/10.1007/s00018-016-2223-0

López LC, Escames G, Tapias V, Utrilla MP, León J, Acuña-Castroviejo D (2006) Identification of an inducible nitric oxide synthase in diaphragm mitochondria from septic mice. Its relation with mitochondrial dysfunction and prevention by melatonin. Int J Biochem Cell Biol 38:267–278. https://doi.org/10.1016/j.biocel.2005.09.008

Lu MC, Ji JA, Jiang ZY, You QD (2016) The Keap1-Nrf2-ARE pathway as a potential preventive and therapeutic target: an update. Med Res Rev 36:924–963. https://doi.org/10.1002/med.21396

Magesh S, Chen Y, Hu L (2012) Small molecule modulators of Keap1-Nrf2-ARE pathway as potential preventive and therapeutic agents. Med Res Rev 32:687–726. https://doi.org/10.1002/med.21257

Marino G, Niso-Santano M, Baehrecke EH, Kroemer G (2014) Self-consumption: the interplay of autophagy and apoptosis. Nat Rev Mol Cell Biol 15:81–94. https://doi.org/10.1038/nrm3735

Martin M, Macias M, Escames G, León J, Acuña-Castroviejo D (2000) Melatonin but not vitamins C and E maintains glutathione homeostasis in t-butyl hydroperoxide-induced mitochondrial oxidative stress. FASEB J 14:1677–1679. https://doi.org/10.1096/fj.99-0865fje

Misra HP, Fridovich I (1972) The role of superoxide anion in the autoxidation of epinephrine and a simple assay for superoxide dismutase. J Biol Chem 247:3170–3175

Mukhopadhyay S, Panda PK, Sinha N, Das DN, Bhutia SK (2014) Autophagy and apoptosis: where do they meet? Apoptosis 19:555–566. https://doi.org/10.1007/s10495-014-0967-2

Neri M, Riezzo I, Pomara C, Schiavone S, Turillazzi E (2016) Oxidative-nitrosative stress and myocardial dysfunctions in sepsis: evidence from the literature and postmortem observations. Mediat Inflamm 2016:3423450–3423412. https://doi.org/10.1155/2016/3423450

Ortiz F, Garcia JA, Acuña-Castroviejo D, Doerrier C, Lopez A, Venegas C, Volt H, Luna-Sanchez M, Lopez LC, Escames G (2014) The beneficial effects of melatonin against heart mitochondrial impairment during sepsis: inhibition of iNOS and preservation of nNOS. J Pineal Res 56:71–81. https://doi.org/10.1111/jpi.12099

Rahim I, Djerdjouri B, Sayed RK, Fernandez-Ortiz M, Fernandez-Gil B, Hidalgo-Gutierrez A, Lopez LC, EscamesG RRJ, Acuna-Castroviejo D (2017) Melatonin administration to wild-type mice and non-treated NLRP3 mutant mice share similar inhibition of the inflammatory response during sepsis. J Pineal Res 63:e12410. https://doi.org/10.1111/jpi.12410

Reiter RJ, Rosales-Corral S, Tan DX, Jou MJ, Galano A, Xu B (2017) Melatonin as a mitochondria-targeted antioxidant: one of evolution's best ideas. Cell Mol Life Sci 74:3863–3881. https://doi.org/10.1007/s00018-017-2609-74

Reynolds ES (1963) The use of lead citrate at high pH as an electron-opaque stain in electron microscopy. J Cell Biol 17:208–212. https://doi.org/10.1083/jcb.17.1.208

Rittirsch D, Huber-Lang MS, Flierl MA, Ward PA (2009) Immunodesign of experimental sepsis by cecal ligation and puncture. Nat Protoc 4:31–36. https://doi.org/10.1038/nprot.2008.214

Rogers GW, Brand MD, Petrosyan S, Ashok D, Elorza AA, Ferrick DA, Murphy AN (2011) High throughput microplate respiratory measurements using minimal quantities of isolated mitochondria. PLoS One 6:e21746. https://doi.org/10.1371/journal.pone.0021746

Sandanger O, Ranheim T, Vinge LE, Bliksoen M, Alfsnes K, Finsen AV, Dahl CP, Askevold ET, Florholmen G, Christensen G, Fitzgerald KA, Lien E, Valen G, Espevik T, Aukrust P, Yndestad A (2013) The NLRP3 inflammasome is up-regulated in cardiac fibroblasts and mediates myocardial ischaemia-reperfusion injury. Cardiovasc Res 99:164–174. https://doi.org/10.1093/cvr/cvt091

Santofimia-Castano P, Clea Ruy D, Garcia-Sanchez L, Jimenez-Blasco D, Fernandez-Bermejo M, Bolanos JP, Salido GM, Gonzalez A (2015) Melatonin induces the expression of Nrf2-regulated antioxidant enzymes via PKC and Ca2+ influx activation in mouse pancreatic acinar cells. Free Radic Biol Med 87:226–236. https://doi.org/10.1016/j.freeradbiomed.2015.06.033

Shi S, Lei S, Tang C, Wang K, Xia Z (2019) Melatonin attenuates acute kidney ischemia/reperfusion injury in diabetic rats by activation of the SIRT1/Nrf2/HO-1 signaling pathway. Biosci Rep 39:BSR20181614. https://doi.org/10.1042/BSR20181614

Singer M (2014) The role of mitochondrial dysfunction in sepsis-induced multi-organ failure. Virulence 5:66–72. https://doi.org/10.4161/viru.26907

Sun J, Ren X, Simpkins JW (2015) Sequential upregulation of superoxide dismutase 2 and heme oxygenase 1 by tert-butylhydroquinone protects mitochondria during oxidative stress. Mol Pharmacol 88:437–449. https://doi.org/10.1124/mol.115.098269

Thimmulappa RK, Lee H, Rangasamy T, Reddy SP, Yamamoto M, Kensler TW, Biswal S (2006) Nrf2 is a critical regulator of the innate immune response and survival during experimental sepsis. J Clin Invest 116:984–995. https://doi.org/10.1172/JCI25790

Tong KI, Kobayashi A, Katsuoka F, Yamamoto M (2006) Two-site substrate recognition model for the Keap1-Nrf2 system: a hinge and latch mechanism. Biol Chem 387:1311–1320. https://doi.org/10.1515/BC.2006.164

Tu W, Wang H, Li S, Liu Q, Sha H (2019) The anti-inflammatory and anti-oxidant mechanisms of the Keap1/Nrf2/ARE signaling pathway in chronic diseases. Aging Dis 10:637–651. https://doi.org/10.14336/AD.2018.0513

Vilhardt F, Haslund-Vinding J, Jaquet V, McBean G (2017) Microglia antioxidant systems and redox signalling. Br J Pharmacol 174:1719–1732. https://doi.org/10.1111/bph.13426

Volt H, Garcia JA, Doerrier C, Diaz-Casado ME, Guerra-Librero A, Lopez LC, Escames G, Tresguerres JA, Acuna-Castroviejo D (2016) Same molecule but different expression: aging and sepsis trigger NLRP3 inflammasome activation, a target of melatonin. J Pineal Res 60:193–205. https://doi.org/10.1111/jpi.12303

Vriend J, Reiter RJ (2015) The Keap1-Nrf2-antioxidant response element pathway: a review of its regulation by melatonin and the proteasome. Mol Cell Endocrinol 401:213–220. https://doi.org/10.1016/j.mce.2014.12.013

Wang J, Jiang C, Zhang K, Lan X, Chen X, Zang W, Wang Z, Guan F, Zhu C, Yang X, Lu H, Wang J (2019) Melatonin receptor activation provides cerebral protection after traumatic brain injury by mitigating oxidative stress and inflammation via the Nrf2 signaling pathway. Free Radic Biol Med 131:345–355. https://doi.org/10.1016/j.freeradbiomed.2018.12.014

Wheeler DS (2011) Oxidative stress in critically ill children with Sepsis. Open Inflamm J 4:74–81. https://doi.org/10.2174/1875041901104010074

Yeh YH, Hsu LA, Chen YH, Kuo CT, Chang GJ, Chen WJ (2016) Protective role of heme oxygenase-1 in atrial remodeling. Basic Res Cardiol 111:58. https://doi.org/10.1007/s00395-016-0577-y

Zador Z, Landry A, Cusimano MD, Geifman N (2019) Multimorbidity states associated with higher mortality rates in organ dysfunction and sepsis: a data-driven analysis in critical care. Crit Care 23:247. https://doi.org/10.1186/s13054-019-2486-6

Zhang DD, Lo SC, Cross JV, Templeton DJ, Hannink M (2004) Keap1 is a redox-regulated substrate adaptor protein for a Cul3-dependent ubiquitin ligase complex. Mol Cell Biol 24:10941–10953. https://doi.org/10.1128/MCB.24.24.10941-10953.2004

Zhao L, An R, Yang Y, Yang X, Liu H, Yue L, Li X, Lin Y, Reiter RJ, Qu Y (2015) Melatonin alleviates brain injury in mice subjected to cecal ligation and puncture via attenuating inflammation, apoptosis, and oxidative stress: the role of SIRT1 signaling. J Pineal Res 59:230–239. https://doi.org/10.1111/jpi.12254

Zhou R, Yazdi AS, Menu P, Tschopp J (2011) A role for mitochondria in NLRP3 inflammasome activation. Nature 469:221–225. https://doi.org/10.1038/nature09663

Zhuang Y, Ding G, Zhao M, Bai M, Yang L, Ni J, Wang R, Jia Z, Huang S, Zhang A (2014) NLRP3 inflammasome mediates albumin-induced renal tubular injury through impaired mitochondrial function. J Biol Chem 289:25101–25111. https://doi.org/10.1074/jbc.M114.57826